SHAPE ESTIMATION OF DEFECTS ON STEAM GENERATOR TUBES

Kozo Shiraishi
Shikoku Research Institute, Inc.
2109-8, Yashimanishi-machi
Takamatsu-shi, Japan

Masanori Izumida and Kenji Murakami
Ehime University
3, Bunkyo-cho
Matsuyama-shi, Japan

INTRODUCTION

Most of the nuclear power plants(NPPs) now in service in Japan are based on either of two reactor technologies – PWR and BWR. While the PWR plant requires steam generators(SG), the BWR plant needs no separate SG because of its capability to produce steam directly. On one hand, the need for installation of SG makes the size of the PWR plant larger than that of the BWR plant, while on the other, separate SG installation offers an advantage in that the controlled area in the PWR plant can be limited, resulting in easier plant maintenance, compared with the BWR plant. Accordingly SG maintenance to preclude radioactive substances from flowing out into the secondary system is one of the most important tasks in operating PWR plants.

Based on this perception, every PWR plant carries out an overhaul of its components, including a full-length inspection of all heat exchanger tubes, during each scheduled outage for refueling. Since some 3,400 heat exchanger tubes are provided for each SG, eddy current testing (ECT) is used for the full-length inspection of the tubes. Assessment of ECT signals is left to visual examination of their forms by skilled analyzers, requiring a very long time for the analysis process.

This paper proposes a method for estimating the depth and volume of defects from these approximate functions [1] and assesses relative errors in the estimated values.

IMITATIVE DEFECTS AND THEIR ECT SIGNALS

In order to facilitate the machining of the tube samples and the calculation of the volume of defects, the shapes of the imitative defects were so set that they could be defined in length l (mm), width w (mm) and depth d (mm) as shown in Figure 1. The tubing material selected for the experiment was an inconel-600 tube with a radius r of 10.48 mm at a point half into the tube wall and a wall thickness D of 1.27 mm. The tube was made to the same specifications as those of heat exchanger tubes now in general use for SG at NPPs.

Review of Progress in Quantitative Nondestructive Evaluation, Vol 17
Edited by D.O. Thompson and D.E. Chimenti, Plenum Press, New York, 1998

A total of 110 imitative defects were prepared with the dimensions l, w and d as specified in Figure 1 and with these dimensions varied as in Table I. In preparing the imitative defects, care was taken to limit the combinations of variable dimensions to those which represent defect shapes similar to actual ones.

Then ECT was conducted with these imitative defects to ECT signals. The signals are assessed by visual examination primarily aimed at finding whether there is any defect in the tube wall from ECT signals as shown in Figure 2. However, the waveforms in these diagrams contain not only necessary information to determine the existence of any defect but also useful information in estimating the shapes of defects detected. We can expect, therefore, that development of technology to accurately estimate the shapes of defects will lead to the improvement of the reliability of a full-length inspection on all heat exchanger tubes and to proper measures for coping with defects found in these tubes. Imitative defects were examined by ECT using only signals at 400 kHz in an effort to solve the problem noted above.

ESTIMATION OF DEFECT DEPTH FROM ECT SIGNALS

The angle between the figure-of-eight Lissajous' pattern in the right diagtram in Figure 2 and the x-axis is defined as the angle of Lissajous' figure θ. Figure 3 shows the relations between θ for each of the 110 ECT signals and the depth d of each of the defects examined. In this diagram, outside, inside and through wall defects are indicated by ■, ●and ▲, respectively, and those which were kept constant in length and width and varied only in depth are connected by solid lines. From the diagram,

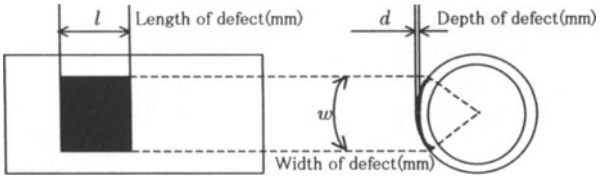

Figure 1. The defect shape by electric discharge machining.

Table I. Shapes of defects.

l	(mm)	0.50	1.00	1.50	2.00	5.00	6.00	8.00 10.00
w	(mm)	0.30	16.46	32.92	49.39	65.85(Full circle)		
d	Outer	0.25	0.51	0.76	1.02	1.27(Through)		
(mm)	Inner	0.25	0.51	0.76	1.02	1.27(Through)		

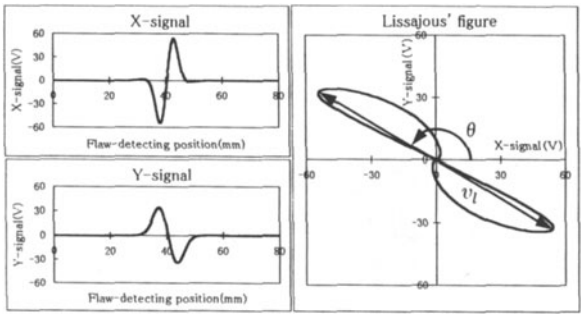

Figure 2. ECT signals.

the findings also indicate that θ contains some errors apparently resulting from the length or width of the defect, but since its depth has a predominant effect, the values of d corresponding to those of θ are distributed roughly on an inverted V-line.

Accordingly use of the relationship described in Figure 3 provides an effective tool to estimate the depth of the defect on which ECT signals can be obtained from θ as well as to find whether the defect is located on the inner or outer surface of the tube wall. Since the number of ECT signals on defects recorded during our test was only 110, the depth of defects was estimated by a leaving-one-out method [2]. More specifically, one of the 110 data was removed and approximate curves of first to fourth orders were determined by the least square error method for the relationship between d and θ in the remaining 109 data. Then the depth of defects in the removed data was estimated from the polynomial.

As stated earlier, the relationship between θ and d shows a line that bends sharply at the point where the region of outside defects meets that of inside defects. Because of great difficulty in approximating this relationship, we decided to divide these curves into two segments at θ_{th}. Figure 4 shows first-to-fourth-order approximations of the relation between θ and d. In this calculation, θ_{th} was set at

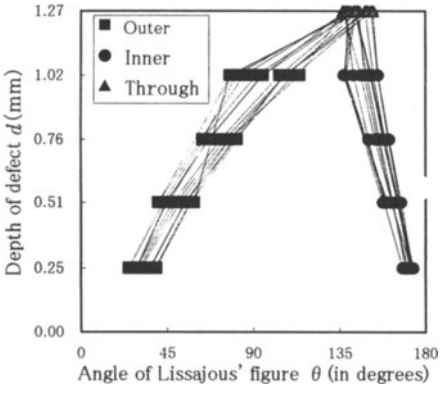

Figure 3. Relation between angle of Lissajous' figure and depth of defects.

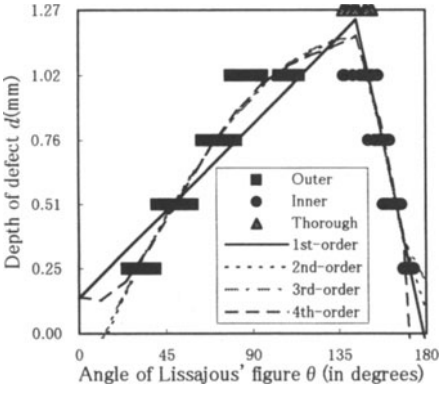

Figure 4. Measured data and approximate curves.

150° where the square error is minimized, and the approximate curves of first to fourth orders are indicated by a solid line, dotted line, alternate long and short dash line, and broken line, respectively. In approximating outer defects ($\theta \leq 150°$), as shown in the diagram, the approximate curves of second and third orders describe roughly the same trajectories, indicating it is likely that points in the part on which no data are provided will follow the relevant data. Table II shows the coefficients of approximate curves of first to fourth orders, for which approximate functions can be written as:

$$d = C_4\theta^4 + C_3\theta^3 + C_2\theta^2 + C_1\theta + C_0 \quad (1)$$

With the coefficients of approximate curves of first to fourth orders in Table II, the depth of defects in the 110 data was estimated from Equation (1) by the leaving-one-out method. From the estimates thus determined, relative errors from true values were calculated in an attempt to find accumulated estimation rates for such errors. The results are shown in Figure 5. From the diagram, the accumulated estimation rate in any of the approximation rose almost linearly over a relative error range of up to 20 %, above which it described a saturation curve.

A close look at an accumulated estimation rate of 80 % found that in the approximations of first to fourth orders, relative errors in 80 % (or 88 in number) of the 110 data could be held down below 26.9 %, 19.7 %, 20.7 % and 23.5 %, respectively. In this instance, the findings indicate, estimation by the second-order approximation attained the best results.

Table II. Coefficients of Approximate Curves.

I/O	Aprroximate curves	C_4	C_3	C_2	C_1	C_0
OD	1st-order	———	———	———	7.58E-03	1.41E-01
	2nd-order	———	———	-6.14E-05	1.87E-02	-2.59E-01
	3rd-order	———	-1.17E-07	-3.06E-05	1.64E-02	-2.07E-01
	4th-order	1.13E-08	-4.01E-06	4.33E-04	-5.92E-03	1.50E-01
ID	1st-order	———	———	———	-3.65E-02	6.52E+00
	2nd-order	———	———	5.37E-04	-2.11E-01	2.06E+01
	3rd-order	———	2.74E-05	-1.28E-02	1.94E+00	-9.53E+01
	4th-order	-1.98E-05	1.28E-02	-3.12E+00	3.37E+02	-1.36E+04

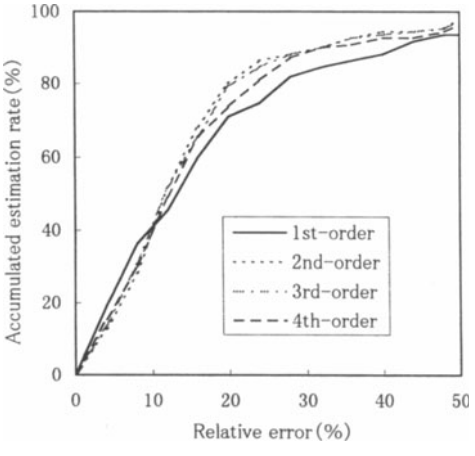

Figure 5. Accumulated estimation rate for relative error of depth estimation of defects.

The length of the Lissajous' pattern in Figure 2 specified as the length of Lissajous' figure v_l(V). Where the wall thickness D of a heat exchanger tube is small enough for the radius r of the tube, the volume of a defect can be written as follows using its length l, width w and depth d:

$$V \simeq lwd \tag{2}$$

The relationship between v_l and V is shown in Figure 6. As indicated in the chart, v_l and V are in almost proportional relation with each other, but since they are distributed widely, approximate functions for these values cannot be derived by the same method as in depth estimation. Except some through defects, however, outer defects are distributed in the upper part of the chart, inner defects in the lower part and through defects in the middle.

Presumably these areas of distribution can be ascribed to the influence of inner and outer defects and their depth. This implies that removal of such influence will make it possible to derive a relational expression for v_l and V.

The magnitude of ECT signals depends on the degree of change in eddy current. In ECT with an inner coil that was used for this study, an eddy current passing through the wall of heat exchanger tubing declines in flow rate as it goes from the inner surface, which is nearer the sensor, to the outer surface as indicated in the drawing. This phenomenon, known as a "skin effect", increases the density of the eddy current as it flows nearer the inner surface of the tube wall and, therefore, the sensor is affected more significantly by inside defects that impede the passage of such high-density current.

From [3], eddy current density $J(z)$ at the depth z from the conductor surface can be written as:

$$J(z) = J_0 \exp(-z\sqrt{\pi f \mu \sigma}) \tag{3}$$

Where
J_0: Current density on the conductor surface(A/mm^2)
f : Frequency of the AC magnetic field (Hz)

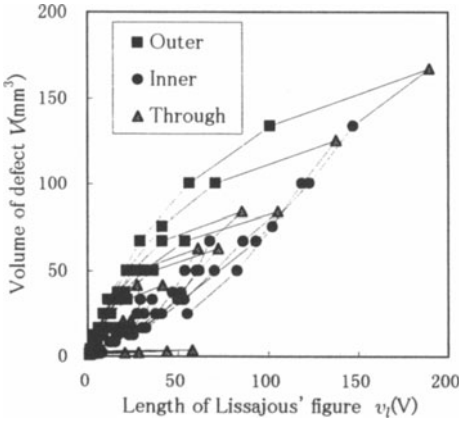

Figure 6. Relation between length of Lissajous' figure and volume of defects.

z : Depth from the conductor surface (mm)
σ : Conductivity of the conductor (S/mm)
μ : Permeability of the conductor (H/mm)

With this equation, the magnitude of the eddy current ie flowing through a space defined by the length l, width w and depth d can be defined as:

$$i_e = \begin{cases} l\dfrac{w}{2\pi r}\displaystyle\int_{D-d}^{D} J(z)\mathrm{d}z & : \text{Outer defect} \\ l\dfrac{w}{2\pi r}\displaystyle\int_{0}^{d} J(z)\mathrm{d}z & : \text{Inner defect} \end{cases} \tag{4}$$

The existence of any defect in this space arrests the flow of the eddy current i_e defined in Expression (4), bringing about a change in the magnetic flux on the periphery of the tube. The extent of such a change in flux $\Delta\phi$(wb) can be written as:

$$\Delta\phi = Mi_e \tag{5}$$

Where M(wb/A) denotes the mutual inductance between the coil around the probe and the heat exchanger tube. The length of Lissajous' figure v_l, which is proportional to the extent of change in the magnetic flux $\Delta\phi$ and occurs as an induced electromotive force, can be given as:

$$v_l \propto \Delta\phi \tag{6}$$

From Expressions (3) through (6), v_l can be approximated as follows at the final stage, using l, w and d:

$$v_l \simeq \begin{cases} Klw(\mathrm{e}^{-\alpha(D-d)} - \mathrm{e}^{-\alpha D}) & : \text{Outer defect} \\ Klw(1 - \mathrm{e}^{-\alpha d}) & : \text{Inner defect} \end{cases} \tag{7}$$

Where K(V/mm^2) is a proportional constant and $\alpha = \sqrt{\pi f \mu \sigma}$(mm^{-1}). The value of α calculated under the test conditions used in this study is 1.30 mm^{-1}. From Expressions (2) and (7), the volume of the defect can be approximated by V' – a calculating expression for v_l and d – as follows:

$$V \simeq V' = \begin{cases} K'v_l\dfrac{d}{(\mathrm{e}^{-\alpha(D-d)} - \mathrm{e}^{-\alpha D})} & : \text{Outer defect} \\ K'v_l\dfrac{d}{(1 - \mathrm{e}^{-\alpha d})} & : \text{Inner defect} \end{cases} \tag{8}$$

Provided $K' = 1/K$. This formula was derived by correcting v_l based on the concept of eddy current density from the conductor surface defined in Expression (3) and, as such, it can clearly identify the relationship between the length of Lissajous' figure and the volume of defects.

Using Expression (8), the volume of defects was estimated by the leaving-one-out method as in estimating their depth. More specifically, the proportional constant K' was determined by the least squares method, using 109 out of the 110 data after removing the one for the defect to be examined. With K', the length of Lissajous' figure v_l and the depth of defects d substituted for the appropriate terms of Expression (8), an attempt was made to determine the estimated value V' for the volume of defects and to calculate its relative error from

the true value V. Since inner and outer defects had to be marked off, as in the case of defect depth estimation, prior to the substitution, we decided to distinguish between these two categories of defects at 140° based on the angle of Lissajous' figure θ.

Figure 7 shows the relationship between the estimated volume of defects V' thus determined and their true volume V. It must be noted here that an estimated value of defect depth determined by the second-order approximation was substituted for the term d in Expression (8). Relations between V' and V, except in the case of some through defects, are distributed diagonally in Figure 7, indicating that the volume of defects, which could not be determined from v_l in Figure 6, can now be estimated using v_l with consideration given to the depth of defects. Those through wall defects which are not distributed on the diagonal line are axial slits. In examining these slit defects, it was found, the estimation of their volume by Expression (8) involves too large an error. Those with their longitudinal axes in the axial direction of the tube provide a longer route for an eddy current to bypass the obstacles. This reduces the eddy current so steeply that the degree of change in its flow rate is reflected in the length Lissajous' figure.

Figure 8 shows the accumulated estimation rate for relative errors in estimated values of defect volume. The solid line indicates the results of calculation with true values substituted for d and the dashed line represents those with estimated values. From the diagram, there is little difference between these two cases of estimation. This means that an error in estimating the volume of defects did not appreciably increase in magnitude from the use for d of estimated values of defect depth with relative errors as described in Figure 5. In examining actual defects in heat exchanger tubes at NPPs, therefore, the volume of defects can be estimated rather satisfactorily using estimated values of defect depth, although true values cannot be substituted for d as they are unknown.

The curves in Figure 8 also indicate that in two cases of which one uses true values for d and the other uses estimated values, relative errors in estimating the volume of defects in 80 % (or 88 in number) of the 110 data can be held down below 36.0 % and 32.1 %, respectively.

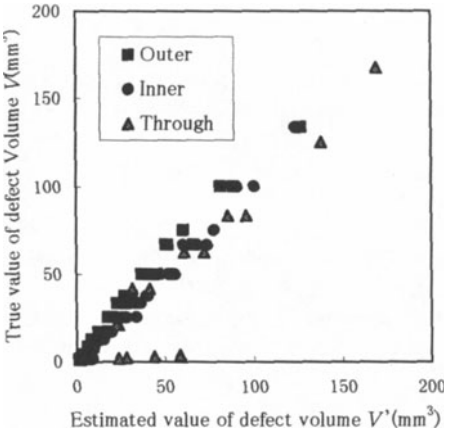

Figure 7. Relation between Estimated and True Values of Defect Volume.

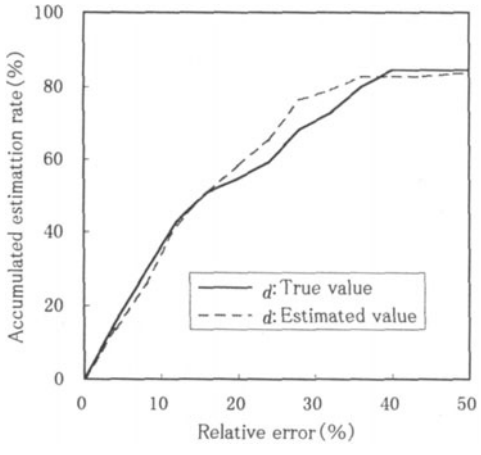

Figure 8. Accumulated Estimation Rate for Relative Errors in Volume Estimation of Defects.

CONCLUSION

This paper proposes a new method that estimates the depth of defects from the angle of ECT signals and the volume of defects from the length of ECT signals with consideration given to the depth of defects, both by approximate functions, using 400-kHz signals from imitative defects made in heat exchanger tubes for SG at NPPs. In estimating the depth of defects, the proposed method uses second-order approximate functions, while in estimating the volume of defects, it uses another form of approximate functions which takes the depth of defects into account. The findings proved that the method can estimate the shapes of defects from the characteristic values of ECT signals by approximate functions.

The proposed method has great potential for application to actual ECT examination at power plants because it can instantly estimate the shapes of defects, uses a clear analysis process and an easy-to-build system, compared with a neural network which requires a long time for learning [4, 5].

REFERENCES

1. K.Shiraishi, M.Izumida and K.Murakami: "Estimation of Defect Shapes from Waveforms of Eddy Current Testing Signals," Shingaku Giho, IE96-40, MVE96-39, pp.41-48 (1996-7)
2. K.Fukunaga: "Introduction To Statistical Pattern Recognition, " ACADEMIC Press (1972)
3. H.Hoshikawa et al: "Eddy Current Testing II," JSNDI (1989)
4. L.Udpa and S.S.Udpa: "Eddy Current Defect Characterization Using Neural Networks," Materials Evaluation, 48, pp342-347 (1990-3)
5. T.Sakai and N.Soneda: "Automatic Recognition of Eddy Current Testing Signals by Neural Network,"Transaction of the JSME, A, Vol.62, No.600, pp.171-177 (1996-8)